
AFRL-AFOSR-VA-TR-2019-0349

# THERMOCHEMISTRY, REACTIVITY, AND DYNAMICS OF METALS ENGAGED IN CHEMIIONIZATION

**Peter Armentrout**
**UNIVERSITY OF UTAH SALT LAKE CITY**

**11/06/2019**
**Final Report**



Air Force Research Laboratory
AF Office Of Scientific Research (AFOSR)/ RTB2
Arlington, Virginia 22203
Air Force Materiel Command

DISTRIBUTION A: Distribution approved for public release.

# REPORT DOCUMENTATION PAGE

*Form Approved*
*OMB No. 0704-0188*



| 1. REPORT DATE *(DD-MM-YYYY)* | 2. REPORT TYPE | 3. DATES COVERED *(From - To)* |
|---|---|---|
| 13-11-2019 | Final Performance | 15 Feb 2016 to 14 Aug 2019 |

**4. TITLE AND SUBTITLE**
THERMOCHEMISTRY, REACTIVITY, AND DYNAMICS OF METALS ENGAGED IN CHEMIIONIZATION

**5a. CONTRACT NUMBER**

**5b. GRANT NUMBER**
FA9550-16-1-0095

**5c. PROGRAM ELEMENT NUMBER**
61102F

**6. AUTHOR(S)**
Peter Armentrout

**5d. PROJECT NUMBER**

**5e. TASK NUMBER**

**5f. WORK UNIT NUMBER**

**7. PERFORMING ORGANIZATION NAME(S) AND ADDRESS(ES)**
UNIVERSITY OF UTAH SALT LAKE CITY
201 PRESIDENTS CIR RM 408
SALT LAKE CITY, UT 84112-9023 US

**8. PERFORMING ORGANIZATION REPORT NUMBER**

**9. SPONSORING/MONITORING AGENCY NAME(S) AND ADDRESS(ES)**
AF Office of Scientific Research
875 N. Randolph St. Room 3112
Arlington, VA 22203

**10. SPONSOR/MONITOR'S ACRONYM(S)**
AFRL/AFOSR RTB2

**11. SPONSOR/MONITOR'S REPORT NUMBER(S)**
AFRL-AFOSR-VA-TR-2019-0349

**12. DISTRIBUTION/AVAILABILITY STATEMENT**
A DISTRIBUTION UNLIMITED: PB Public Release

**13. SUPPLEMENTARY NOTES**

**14. ABSTRACT**

The exothermicity of the chemi-ionization reaction M + O MO+ + e has been re evaluated for M = Sm, Gd, and Nd. Guided ion beam tandem mass spectrometry (GIBMS) has been used to determine the bond dissociation energies (BDEs) of MO+ for all three metals, as determined by the observed reactivity of M+ and MO+ with several species. Combined with the established M ionization energies, these BDEs allow re-evaluation of the exothermicities of the chemi-ionization reactions. Implications of these results for interpretation of chemical release experiments in the thermosphere were evaluated. In addition, GIBMS work has also examined reactions of Sm+ with CO2 and OCS to form SmO+ and determined that these reactions exhibit barriers to their formation, which has been shown by theory to result from the need to couple the ground state surfaces of Sm+ (8F1/2,4f66s1) to an electronic surface evolving from the 13/2 (4f55d6s) excited state. Studies of the reactions of M+ with H2, HD, and D2 (M = Sm and Gd) allowed BDEs of the metal hydride cations to be measured. In addition, reactions of Sm+ and SmS+ with sulfur donors allowed the SmS+ BDE to be determined and compared to advanced computational results. Potential energy surfaces for [Gd,2O]+ and [Gd,C,2O]+ systems were been evaluated experimentally. The BDE of Au2+ has been measured and its reactivity with methane (previously reported to show catalytic formation of ethene) has been studied shown not to exhibit the aforementioned catalytic behavior. Oxidation of iron carbonyl cations has also been examined.

**15. SUBJECT TERMS**
lanthanide, chemiionization, samarium

**16. SECURITY CLASSIFICATION OF:**

Standard Form 298 (Rev. 8/98)
Prescribed by ANSI Std. Z39.18

| a. REPORT | b. ABSTRACT | c. THIS PAGE | 17. LIMITATION OF ABSTRACT | 18. NUMBER OF PAGES | 19a. NAME OF RESPONSIBLE PERSON |
|---|---|---|---|---|---|
| Unclassified | Unclassified | Unclassified | UU | | BERMAN, MICHAEL |
| | | | | | 19b. TELEPHONE NUMBER *(Include area code)* 703-696-7781 |

**Final Report**

Project Title: THERMOCHEMISTRY, REACTIVITY, AND DYNAMICS OF METALS ENGAGED IN CHEMI-IONIZATION


| | |
|---|---|
| Institution: | University of Utah,<br>Department of Chemistry |
| Street Address: | 315 South 1400 East, Room 2020<br>Salt Lake City, UT 84112-0850 |
| Principal Investigator: | Peter B. Armentrout |
| Address: | Department of Chemistry<br>University of Utah<br>315 South 1400 East, Room 2020<br>Salt Lake City, UT 84112-0850 |
| Telephone Number: | (801) 581-7885 |
| Email: | armentrout@chem.utah.edu |



Funding Opportunity Announcement Number: BAA-AFOSR-2014-0001

CFDA 12.800 CID RTE-4

Air Force Office of Scientific Research
Energy, Power and Propulsion Sciences (RTE)
Molecular Dynamics and Theoretical Chemistry (RTE-4)

Program Officer: : Dr. Michael R. Berman AFOSR/RTE (703) 696-7781
DSN 426-7781; FAX (703) 696-7320
E-mail: michael.berman@us.af.mil

AFOSR Grant Number: FA9550-16-1-0095

THERMOCHEMISTRY, REACTIVITY, AND DYNAMICS OF METALS ENGAGED IN CHEMI-IONIZATION

Principal Investigator: Peter B. Armentrout (armentrout@chem.utah.edu)
Institution: University of Utah, Department of Chemistry
Salt Lake City, UT 84112-0850

Funding Opportunity Announcement Number: BAA-AFOSR-2014-0001; CFDA 12.800

Air Force Office of Scientific Research; Energy, Power and Propulsion Sciences (RTE)
Molecular Dynamics and Theoretical Chemistry (RTE-4)

Program Officer: Dr. Michael R. Berman AFOSR/RTE (michael.berman@us.af.mil)

**I. Statement of Objectives**

The Air Force has explored the possibility of using chemi-ionization reactions of atomic metals with oxygen atoms in the ionosphere as a means to form enhanced plasma densities in the atmosphere, which are one potential means to mitigate scintillation effects that interfere with satellite communications. Underscoring the need for fundamental information regarding such reactions are atmospheric release studies involving samarium, which failed to proceed as expected. This failure demonstrated that the literature data regarding the thermodynamics, reactivity, and dynamics of oxidation of samarium (and other lanthanides) was inaccurate.

To acquire more accurate information on lanthanide oxidation, reactions of the atomic metal cations and their oxides with atmospheric gases (e.g., $O_2$, CO, $CO_2$) as well as collision-induced dissociation (CID) of the metal oxide cations (and in some cases, their reactivity) has been studied as a function of kinetic energy in a guided ion beam tandem mass spectrometer (GIBMS). Such reactions are of direct interest in understanding the chemistry of lanthanides exposed to the atmosphere at high temperature. Analysis of the kinetic energy dependent data has provided quantitative bond energies of a variety of species yielding a better fundamental understanding of the chemical and physical properties of these metals. Both the kinetic and thermodynamic data should be useful in modeling and predicting the chemistry of these species in the atmosphere and other venues, such as catalysis. Furthermore, because such heavy metals exhibit extensive spin-orbit interactions, exploration of these systems and their periodic trends has provided fundamental information needed to better understand and model these chemistries.

Accurate quantum chemical calculations on heavy metal species are particularly problematic because they require consideration of relativistic effects under conditions where electron correlation is also of great importance. The challenges of these calculations are exacerbated by a shortage of accurate quantitative information on such heavy metal molecules, which makes validation of any approximations employed difficult. One aim of the work presented here is to determine accurate thermochemical data that can be used as benchmarks for these advanced quantum chemical methods. Routine comparisons have been conducted in house, but collaborations with Prof. Kirk Peterson of Washington State University and Prof. Hua Guo of the University of New Mexico has permitted evaluations of state-of-the-art computational methods.

Accompanying its scientific merit is the fact that this work has involved the education of graduate and undergraduate students in lanthanide science and experiments.

## II. Research Effort

The reactivity and thermochemistry of metal atoms that potentially undergo the chemi-ionization reaction 1 was characterized using guided ion beam tandem mass spectrometry

$$M + O \rightarrow MO^+ + e^- \qquad \Delta H < 0 \text{ kJ/mol} \qquad (1)$$

(GIBMS) experiments. Thermodynamic information about cationic and neutral species of direct interest to the Air Force was obtained, as demonstrated below. In addition, the systems studied have extensive spin-orbit interactions, with effects on the reactivity and thermodynamics that are not well understood. Exploration of these systems provided opportunities to reveal the dynamics of such systems, yielding information that provides a better understanding of fundamental aspects of the atmospheric and catalytic chemistry of heavy metals. Related theoretical calculations synergistically enhanced the experimental studies.

Augmenting these studies of the lanthanides were collaborative efforts to assist the plasma chemistry group at the Air Force Research Laboratory (AFRL) in their efforts to more completely understand metal based chemistry and catalysis. Our work in these areas over the past funding period can be found in refs. [1-14].

### A. Background

Satellite communications (e.g., global positioning systems, GPS, and telecommunications) are of clear importance in both the civilian and military sectors. Scintillation, caused by natural irregularities in the ionosphere, can interfere with radio wave propagation leading to intermittent or complete loss of communication. In critical applications, it may be desirable to mitigate scintillation by directly inducing man-made enhanced plasma densities to slow the growth of the ionospheric instabilities. The Air Force has explored the possibility of creating such artificial plasma clouds by increasing the electron and cation densities using chemical release. Materials such as barium, strontium, xenon, lithium, and cesium have been studied, but require solar photons or particle collisions for ionization, hence limiting their efficiency. Another process that holds promise in this regard is chemi-ionization (CI), in particular, reaction 1 where M is an elemental metal. For this reaction to be exothermic, the bond dissociation energy (BDE) of MO, D(MO), must exceed its ionization energy, IE(MO), which is highly unusual. Thus, IE(MO) must be low (a metal is essentially required) and the bond being formed must be strong, a triple bond is needed. These two requirements are fulfilled when M is an early transition metal, lanthanide, or actinide.

If the CI reaction 1 is exothermic, it can occur spontaneously by utilizing the atomic oxygen present at the altitudes of interest, ~170 km. Further, the undesirable reverse reaction, which has a very large cross section because of Coulomb attraction, is inefficient because it is endothermic. (This simplistic conclusion is mediated by the fact that the electron temperature in the ionosphere is ~1000 K, such that an appreciable fraction of energetic electrons can undergo the reverse process if reaction 1 is not exothermic by more than ~0.4 eV.) AFRL Metal Oxide Space Cloud (MOSC) experiments were conducted to test the formation of an artificial plasma cloud by this process using samarium, M = Sm.[15] Samarium was chosen for these initial experiments because the literature indicated the reaction was exothermic by ~0.3 eV,[16] and Sm has a relatively low boiling point (2067 K,[17] 2173 K[18]), such that a titanium-boron thermite mixture reaching temperatures of ~3500 K would efficiently vaporize this material. Predictions suggested that a few kg of Sm dispersed in the ionosphere could create an enhanced plasma cloud over distances extending as far as 100 km. Unfortunately, the plasma density produced was one-two orders of magnitude smaller than expected, and the cloud shape and color differed significantly from pre-launch predictions.

To understand these phenomena, the plasma chemistry research group of Dr. Albert Viggiano at AFRL was contacted to explore the chemistry of samarium more thoroughly. Using their selected ion flow tube (SIFT) apparatus equipped with an electrospray ionization (ESI) source, they determined the rates and temperature dependences of several reactions of $Sm^+$ and $SmO^+$ near room temperature, finding that $N_2O$, $NO_2$, $O_2$, and $SO_2$ all react with $Sm^+$ to form $SmO^+$.[1] The thermochemistry in Table 1 shows that these observations suggest that $D(Sm^+\text{-}O) > 5.66$ eV = D(OS-O). In contrast, the SIFT studies also found that $CO_2$ and NO were unreactive with $Sm^+$. Because D(OC-O) is lower than 5.66 eV, the failure to react with $CO_2$ at room temperature cannot be a consequence of unfavorable thermodynamics, but rather must result from kinetic effects. In addition, the SIFT studies determined that $SmO^+$ reacted with $N_2O$, $NO_2$, $O_2$, $CO_2$, $SO_2$, and NO exclusively by three-body association. Unfortunately, these data yielded no specific insight into the MOSC results, hence, the PIs laboratory was contacted to see if we could elucidate the thermochemistry of SmO and $SmO^+$ more thoroughly.

Table 1:
Oxide Bond Energies

| Species | $D_0$(M-O), eV |
|---|---|
| $N_2O$ | 1.667 ± 0.001 |
| $NO_2$ | 3.116 ± 0.001 |
| $H_2O$ | 5.035 ± 0.001 |
| $O_2$ | 5.117 ± 0.001 |
| $CO_2$ | 5.453 ± 0.001 |
| $SO_2$ | 5.661 ± 0.014 |
| NO | 6.496 ± 0.001 |
| SCO | 6.88 ± 0.04 |
| CO | 11.111 ± 0.001 |

As described further below, the GIBMS approach developed in the PIs laboratory has proven to be a versatile experimental method of determining quantitative thermodynamic information. During the last funding cycle, the PI's group studied several reactions that provided specific information regarding $D(SmO^+)$, with the results published early in the last funding cycle.[1] These data provided a substantially lower BDE than the literature, sufficiently so that reaction 1 is actually exothermic by only 0.08 ± 0.07 eV, thereby permitting the dissociative recombination reverse reaction to occur with about 80-90% of the electrons available, lowering the anticipated plasma density. Simulations of the MOSC test using this thermodynamic information are in agreement with the experimental results from this test,[15, 19] thereby confirming the utility of the fundamental thermodynamic data provided by the PIs laboratory. In addition, we have also provided similar data for two more lanthanide oxide cations, $GdO^+$ and $NdO^+$,[3, 12] as well as performing additional explorations of the oxidation and hydrogenation chemistry of $Sm^+$, $Gd^+$, and $Nd^+$,[4-6, 8-11] along with several studies that augment studies by Viggiano's AFRL group.[2, 7, 13-14]

**B. Experimental methods**

**Overview**. The experimental technique we use is GIBMS.[20-23] This device uses mass spectrometry to select an ionic reactant, which reacts under single collision conditions with neutral molecules in a radiofrequency (rf) octopole ion beam guide, and then analyzes the products using mass spectrometry, with single molecule sensitivity. The two Utah GIBMS instruments allow the study of the kinetic energy dependence of ion-molecule reactions over a wide (four order of magnitude) energy range. This enables the measurement of the thermodynamics of metal-ligand interactions using two types of processes: exchange reactions 2,

$$M^+ + LR \rightarrow ML^+ + R \qquad (2)$$

and collision-induced dissociation (CID), reactions 3.

$$ML_x^+ + Xe \rightarrow ML_{x-1}^+ + L + Xe \qquad (3)$$

If the reaction in the first case is endothermic, the reaction threshold, $E_0$, can be measured and related to the BDE of $M^+$-L by $D_0(M^+\text{-}L) = D_0(LR) - E_0$, with $D_0(LR)$ taken from the literature (e.g., Table 1). In the intrinsically endothermic CID process, $E_0$ equals $D_0(L_{x-1}M^+\text{-}L)$ as long as there are no barriers to the reverse process, which is generally true because of the long-range

attraction between ions and polarizable and polar molecules.[24] Accurate determination of BDEs using this approach requires that several factors be taken into account, as detailed below.[22-24]

**Ion generation.** The ion source is a critical feature for the quantitative study of the energetics of ion-molecule reactions. Unless the internal energy of the ions is adequately controlled, our knowledge of the energy available to reaction and thus the precision and accuracy of any thermodynamic measurement is compromised. For the studies proposed here, this control is achieved using a dc discharge/flow tube (DC/FT) source.[21, 25-30] This source has been used to generate atomic metal and metal oxide ions for studies of reactions 2 and 3 with most of the transition metals (TMs), measuring a wide variety of covalent metal-ligand bonds.[31-32] It is also the source used in the lanthanide chemistry outlined below, as well as recent work on the actinide thorium.[33-38] In this source, argon (about 10% in He) is ionized by a kV dc potential and then collides with the cathode composed of or containing the material of interest, sputtering the desired metal cations. Ions generated in this glow discharge can then undergo further reaction (such as oxidation or condensation) in the meter-long flow tube. In addition, the ions are thermalized by undergoing about $10^5$ collisions with the inert flow gases. For atomic transition metal cations, we have demonstrated that the distribution of electronic states produced by the DC/FT source is usually thermal or nearly so. (In the few cases where excited electronic states are produced,[39-47] these are easily removed by adding quench gases to the flow.) By comparing results with those from a surface ionization source (where the source temperature is known), the DC/FT source has been shown to generate $Sc^+$,[48] $Fe^+$,[49] $Co^+$,[50] $Ni^+$,[51] $Ru^+$, $Rh^+$, and $Pd^+$ [52] ions with average electronic temperatures of 700 ± 400 K, and $Y^+$, $Zr^+$, $Nb^+$, and $Mo^+$ ions with average electronic temperatures of 300 ± 100 K.[53] Therefore, we conservatively quote the DC/FT source temperature as 700 ± 400 K. Thus, for lanthanide cations, the dominant electronic state occupied is the ground state term.

The DC/FT source can produce species such as $M^+$, $MO^+$, and $MO_2^+$. Termolecular reactions can attach one or many ligands of all sorts (Ar, CO, $N_2$, $H_2O$, $CO_2$, amino acids, through crown ethers) to bare metal and oxygenated ions throughout the periodic table,[26-27, 29-30, 54-56] thereby generating a wide range of $ML_x^+$ species. Using reactions 3, quantitative measurements of noncovalent metal-ligand interactions have been examined for alkali, alkaline earth, and transition metal ions with a wide range of ligands.[31-32, 56] Below, such studies are illustrated by determination of the BDEs of $M^+$–O, $M^+$–$CO_2$, $OM^+$-CO (where M = Sm and Gd),[6, 9] and $Gd^+(O_2)$.[5]

**Guided ion beam mass spectrometry.** Once the ions leave the source, they pass through a differentially pumped chamber where they are focused into a beam and mass analyzed. They then enter another chamber, where they are decelerated to a desired kinetic energy and injected into an rf octopole beam guide,[57] which acts as a radial ion trap. The octopole passes through a reaction cell containing a neutral reactant gas maintained at sufficiently low pressure that single-collision conditions prevail. The pressure dependence of all cross sections is measured to ensure that rigorous single-collision conditions are used in the data analysis. Product and remaining reactant ions drift to the end of the octopole, where they are focused into a final differentially pumped chamber. (In one instrument, the octopole region contains two octopoles, which allows additional dynamics experiments to be conducted.[58]) Here, the ions are separated with a quadrupole mass filter and detected using a secondary electron scintillation (Daly) detector[59] and standard ion pulse counting techniques that provide essentially unit detection capability up to high masses. Data collection is under computer control, which allows extensive signal averaging. At each relative kinetic energy, $E$, the intensities of transmitted reactant and product ions are converted to absolute reaction cross sections for each product channel, $\sigma(E)$.[20] These cross sections have absolute uncertainties of ±20%. Relative cross sections are accurate to about ±5%.

There are several advantages to using GIB techniques to study ion-molecule reactions. First, the range of energies available to the instrument is extensive, four orders of magnitude ranging from thermal to a thousand electron volts. This is the primary distinction between the GIBMS and other instrumentation for studying ion-molecule reactions, which is generally limited to thermal energies. Second, the absolute kinetic energy scale can be determined accurately using the octopole as a highly efficient retarding energy analyzer. Third, the octopole ion beam guide allows for efficient product collection.[20, 58, 60] Fourth, the octopole extends well beyond the ends of the gas cell (unlike those of triple quadrupoles) such that the collision energy is well-controlled and the $1/r^6$ effective potential is much less perturbing than the $1/r^2$ potential of quadrupoles.

**Data analysis.** The ability to examine reactions over a very wide range of kinetic energies is the distinguishing and truly powerful ability of GIB methods. This capability allows endothermic reactions to be examined routinely. By measuring the threshold for reactions 2 or 3, we obtain thermodynamic information for a wide variety of species. This assumes that activation barriers exceeding the endothermicity are not present, which is generally valid because of the long-range attractive form of ion-molecule interactions,[24, 61] provided there are no constraints resulting from spin or orbital angular momentum conservation.[23] (Interestingly, the samarium chemistry discussed below provides several examples of such unusual constraints.) For CID studies involving heterolytic bond cleavages, which encompasses some systems of interest here, we have shown that there should be no reverse activation barriers because of electronic considerations.[24]

Our methods of analysis have been amply described in the literature,[22-23] and have proven to be robust. Briefly, Eq. 4 is used to reproduce the energy dependence of reaction cross sections.

$$\sigma(E) = \left(\frac{n\sigma_o}{E}\right)\sum_i g_i \int_{E_o - E_i}^{E} (1 - e^{-k(\varepsilon + E_i)\tau})(E - \varepsilon)^{n-1} d\varepsilon \qquad (4)$$

$\sigma_0$ is an energy independent scaling factor, $E$ is the relative translational energy, $E_0$ is the reaction threshold at 0 K, and $n$ is an adjustable fitting parameter that describes the efficiency of the energy transfer upon collision.[58] The summation is over the rovibrational and electronic states of the reactants having excitation energies, $E_i$, and populations, $g_i$, where $\Sigma g_i = 1$. $\varepsilon$ represents the energy deposited into the ion upon collision with the neutral reagent, such that the energy available to the energized molecule (EM) is $E^* = \varepsilon + E_i$. $\tau$ is the average timescale of the experiment (ion time-of-flight from the collision cell to the quadrupole mass spectrometer, either ~0.1 or 0.5 ms for the single and dual octopole instruments, respectively). $k(\varepsilon + E_i) = k(E^*)$ is the Rice-Ramsperger-Kassel-Marcus (RRKM) unimolecular dissociation rate constant[62-63] as calculated using Eq. 5,

$$k(E^*) = sN^{\dagger}_{vr}(E^* - E_0) / h\rho_{vr}(E^*) \qquad (5)$$

where $s$ is the reaction degeneracy calculated from the ratio of rotational symmetry numbers of the reactants with respect to the products, $N^{\dagger}_{vr}(E^* - E_0)$ is the sum of the rovibrational states of the transition state (TS) at an energy $E^* - E_0$ above the threshold, and $\rho_{vr}(E^*)$ is the density of rovibrational states for the EM. When the rate constant is much faster than $\tau$ (which is generally true for small molecular systems), Eq. 4 reduces to a simple modified line-of-centers form, Eq. 6.

$$\sigma(E) = \sigma_0 \sum g_i (E + E_i - E_0)^n / E \qquad (6)$$

This form is often sufficient to analyze the cross sections for exchange reactions 2. After convolution over the kinetic energy distributions of both reactants, Eqs. 4 and 6 have been shown to accurately describe the kinetic energy dependence of many bimolecular reactions and CID experiments (see examples below in Figs. 2 – 4).

This model for the kinetic energy dependence of ion-molecule reactions includes explicit consideration of the internal energy of both reactants,[20, 64-66] and has been shown to be directly compatible with direct measurements of the energy transfer function.[58] For CID of larger systems, the model includes the possibility that the collisionally excited complex does not dissociate during the experimental flight time, which can lead to a delayed onset for the CID threshold, a kinetic shift. Our model includes an estimate of this effect by incorporating statistical (RRKM) rate theory for the unimolecular dissociation rate of an EM.[67-68] Several reasonable treatments of the assumed energy and angular momentum distributions of the collisionally-activated molecules were considered. This statistical approach also allows a straightforward introduction of competing dissociation channels,[69] for which results demonstrate that a statistical model for the rotational energy distributions gives the most accurate thermodynamic data. Additional work shows that the best results may require explicit handling of internal rotations.[70] These statistical analysis methods have been extensively tested and further developed.[71-76] These studies demonstrate that a phase space theory (PST) approach in which rotational and orbital angular momentum are explicitly conserved and allowed to interchange provides the best reproduction of the data, however, they also demonstrate that the thermodynamic information obtained is insensitive to the assumptions regarding angular momentum. Overall, the model has been shown to reproduce the threshold regions of a variety of endothermic ion-molecule reactions, including CID, with good accuracy in the resulting thermochemistry. Recent efforts have now extended our "toolbox" of thermodynamic methodology from simple bimolecular reactions and CID, to variants involving competitive[69] and sequential dissociation pathways,[77] as well as to association[75] and ligand exchange reactions.[76] These methods therefore allow multiple pathways for obtaining and verifying accurate BDEs, as well as free energies and entropies. Although the precision of such measurements does not approach spectroscopic analogues, it is nevertheless still quite good, often 0.1 eV or less (as for example for $SmO^+$, $GdO^+$, and $NdO^+$), and occasionally as low as 0.02 eV.[78]

**C. Previous related works**

As illustrated below, for all of the reactions we study, we determine absolute reaction cross sections that are direct measures of ion reactivity and can be converted to rate constants over broad ranges of temperature, e.g., see ref. [14] (although the kinetic and internal energies of the reactants are no longer equilibrated). In addition to quantitative thermodynamic information, the kinetic energy dependences provide insight into the reaction mechanisms. Most studies referred to in this section include quantum chemical calculations,[1, 3, 5-6, 8-12, 44-47, 78-95] which provide details about the structures of the species formed and the potential energy surfaces (PESs) of the reactions.

**Reactions involving samarium. Chemi-ionization thermochemistry.** Our work on samarium shows that the lanthanide systems provide interesting and surprising results that are not completely understood, and therefore suggest additional studies. The literature regarding the BDE of SmO, $D_0(SmO)$, was reviewed thoroughly in our recent paper.[1] Several high temperature studies yielded BDEs with a range of $5.5 \pm 0.2 - 6.10 \pm 0.03$ eV[96-98] and have been analyzed in several compilations.[99-103] The most inclusive and conservative value is $5.88 \pm 0.17$ eV.[100] The ionization energy of SmO, IE(SmO), was measured using electron ionization and high temperature mass spectrometry (HTMS) as $5.55 \pm 0.1$ eV.[104] Thus, the enthalpy of reaction 1, $\Delta H_0(1) = IE(SmO) - D_0(SmO)$, can be determined as $5.55 - 5.88 = -0.33 \pm 0.20$ eV. Because $IE(MO) - D_0(MO) = IE(M) - D_0(MO^+)$, these data also indicate that $D_0(Sm^+–O) = 5.97 \pm 0.20$ eV given IE(Sm) = 5.6437 eV.[105] This BDE is consistent with the SIFT studies of the AFRL laboratory that reaction of $Sm^+$ with $N_2O$, $NO_2$, $O_2$, and $SO_2$ were all exothermic in forming $SmO^+$, as well as the lack of reaction with

NO as it is endothermic (Table 1).[1] However, this BDE also indicates that reaction with $CO_2$ is exothermic, whereas no reactivity was observed at thermal energies between $Sm^+$ and $CO_2$ in the AFRL SIFT studies.[1]

In our GIBMS studies of $Sm^+$, the ions were generated using the DC/FT source. For $Sm^+$, an electronic temperature of 700 ± 400 K means that 21 – 68 % of the ions are in their ground $^8F_{1/2}$ level with 27 – 34% in the $^8F_{3/2}$ level at 0.04 eV, and 4 – 21% in the $^8F_{5/2}$ level at 0.104 eV.[106] Overall, the average electronic energy is 0.06 ± 0.05 eV, an uncertainty that is included in our determination of the threshold energies. Our results for reaction of $Sm^+$ with $O_2$, $SO_2$, $CO_2$, and NO agreed with the AFRL findings. Reactions of $Sm^+$ with both $O_2$ and $SO_2$ efficiently form $SmO^+$ with cross sections exhibiting no barrier as low in energy as we can go (~0.015 eV), indicating that $D_0(SmO^+) > D_0(O_2)$ and $D_0$(OS-O). Reaction efficiencies were 100 ± 20% and 22 ± 4%, respectively, in reasonable agreement with the AFRL SIFT studies. GIBMS studies of the $Sm^+ + CO_2$ reaction show that formation of $SmO^+$ exhibits a barrier, consistent with the AFRL SIFT experiments. Because $D_0$(OC-O) < $D_0$(OS-O), Table 1, the formation of $SmO^+$ in the $Sm^+ + CO_2$ reaction must be exothermic, such that the observed barrier must originate from some other feature of the reaction system. *Such a barrier is unusual in ion-molecule chemistry and its exploration should reveal interesting electronic properties of lanthanide chemistry (see next section).*

In order to determine a more precise value for $D_0(SmO^+)$, we examined several reactions that the AFRL group could not profitably study at thermal energies, including $Sm^+ + CO$, $SmO^+ + Xe$, and $SmO^+ + O_2$. (Reaction of $SmO^+ + O_2$ also forms $SmO_2^+$ in an endothermic process that allows $D_0(OSm^+\text{-}O) = 1.14 \pm 0.15$ eV to be measured.[1]) For reaction with CO, we measured a threshold for $SmO^+$ production of 5.49 ± 0.15 eV, which combined with $D_0$(CO), Table 1, yields $D_0(SmO^+) = 5.62 \pm 0.15$ eV, consistent with the exothermic reaction of $Sm^+ + O_2$ and $SO_2$ within experimental uncertainty. In the CID reactions of $SmO^+$ with Xe and $O_2$, the thresholds measured are 5.67 ± 0.16 and 5.78 ± 0.09 eV, respectively. These values should directly correspond to $D_0(SmO^+)$, although conservatively they are upper limits as the translational to internal energy transfer can be inefficient for strongly bound species like $SmO^+$. Notably, these three BDEs are within experimental uncertainty of each other and have a weighted average of $D_0(Sm^+\text{-}O) = 5.72_5 \pm 0.07$ eV (one standard deviation).[1] This value agrees with the best literature value, 5.97 ± 0.20 eV, within combined experimental uncertainties, but is more precise and lower by 0.25 eV.

An important test of this value was also reported in our recent work.[1] The group of Prof. M. Heaven (Emory U.) measured IE(SmO) using pulsed-field ionization zero kinetic energy (PFI-ZEKE) photoelectron spectroscopy. Their final result, 46318 ± 5 $cm^{-1}$ (5.7427 ± 0.0006 eV), is 0.19 eV higher than the literature value of 5.55 ± 0.1 eV.[104] In previous work,[85, 107-108] the IEs reported by Rauh and Ackermann[104, 109] for ZrO, HfO, and TaO have also been found to be too low by even larger amounts. This systematic difference may occur because the population of excited states at the elevated temperatures used in these early experiments was not adequately accounted for. Combined with the literature value for $D_0(SmO) = 5.88 \pm 0.17$ eV and IE(Sm) = 5.6437 ± 0.0006 eV, this refined IE(SmO) yields $D_0(SmO^+) = 5.78 \pm 0.17$ eV, in agreement with the more precise GIBMS value. Conversely, combining these very precise IEs with our value for $D_0(SmO^+)$ yields a refined neutral BDE of $D_0(SmO) = 5.83 \pm 0.07$ eV.

Finally, we return to the enthalpy for the chemi-ionization reaction 1. According to our measurements, the $SmO^+$ bond energy is $5.72_5 \pm 0.07$ eV (weighted average of three values). Given this value and IE(Sm), the CI reaction 1 is exothermic by 0.08 ± 0.07 eV, 0.25 eV lower than previously thought. Recent models of the MOSC test using this thermochemistry have nicely accounted for the observations made in the atmospheric tests but suggest that excited states of Sm

could enhance the CI reaction, such that the electron density could be affected by photoionization and photo-excitation.[19] This result is also consistent with the original observations of Fite and coworkers,[110] Dyke and coworkers,[111] and more recent AFRL studies[112] that the CI process with samarium is observed but with relatively small probabilities.

**Reactions of samarium. Atomic orbital diabaticity**. As we examined the chemistry of samarium, it became evident that lanthanides may be interesting catalytic metals because f-orbitals are potentially both sources and sinks (temporary storage) for electron density, thereby allowing flexibility in the number of valence electrons available for catalytic transformations. In considering this possibility, it becomes important to understand any limitations on movement of electrons between the 4f-orbitals (which do not engage in bonding) and the active 6s, 6p, and 5d-orbitals. Generally, conservation of spin would not be considered to be a limitation for such heavy metals.

As noted above, observation of a barrier for reaction of $Sm^+$ with $CO_2$ is a result that we thought needed to be understood more thoroughly, both experimentally and computationally. Further, our GIBMS studies of the reactions of $Sm^+$ with OCS and NO also exhibited thresholds for $SmO^+$ formation that exceeded the endothermicities of these reactions, presumably induced by similar limitations as the $CO_2$ system. To explore the $CO_2$ reaction more completely, we examined the reverse reaction, $SmO^+ + CO \rightarrow Sm^+ + CO_2$, finding that the onset for production of $Sm^+$ had a threshold energy consistent with the measured barrier height of the forward reaction, $1.77 \pm 0.11$ eV, combined with the calculated exothermicity of this reaction, $D_0(Sm^+\text{-}O) - D_0(OC\text{-}O) = 5.72_5 - 5.45_3$ eV $= 0.27 \pm 0.07$ eV, i.e., a reverse barrier height of $2.04 \pm 0.13$ eV. This result unambiguously shows that there is a barrier in excess of the product asymptotes for both forward and reverse reactions. At higher collision energies, the cross section for formation of $Sm^+$ increases sharply above ~ 6 eV, which can be attributed to CID (formation of $Sm^+ + O + CO$), as demonstrated by the magnitude and shape of the cross section being similar to those found in the CID reactions with Xe or $O_2$. (Fig. 3 below shows this for the analogous reactions of $NdO^+$.)

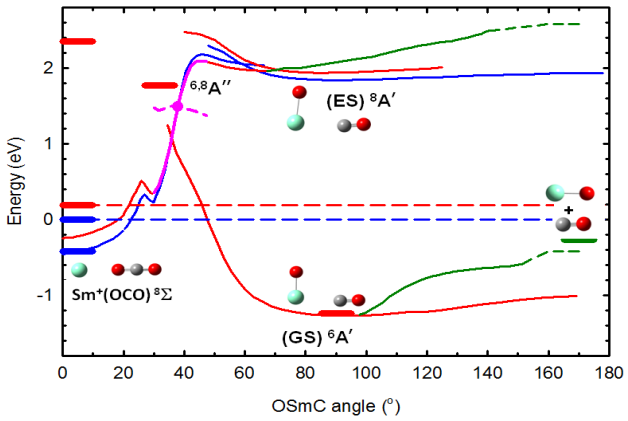


**Fig. 1.** Calculated PESs versus the OSmC bond angle for reaction of $Sm^+$ with $CO_2$ corrected for the SO splitting of $Sm^+(^8F_{1/2})$. Red and blue lines indicate surfaces of sextet and octet spin, respectively. Thick short horizontal lines show experimentally determined energies. Green lines show dissociation to the $SmO^+ + CO$ asymptote. The dashed pink line shows the sextet surface for a $4f^5$ electron configuration at the same geometries as those with six 4f electrons (solid pink line), with the CP indicated by the pink circle.

We also examined the CID reactions of $Sm^+(CO_2)$ and $OSm^+(CO)$, species that are easily formed in the flow tube source by attaching the $CO_2$ or CO molecules to $Sm^+$ and $SmO^+$ using three-body association reactions. These experiments establish well depths of $D_0(Sm^+\text{-}CO_2) = 0.42 \pm 0.03$ eV and $D_0(OSm^+\text{-}CO) = 0.97 \pm 0.07$ eV. (BDEs for two and three $CO_2$ ligands on $Sm^+$ were also measured.) Thus, five points along the $Sm^+ + CO_2$ PES (reactants, products, two intermediates, and the barrier height) were experimentally established. These are shown in Fig. 1 (thick horizontal lines) along with our theoretical PESs: MP2 level with Stuttgart Dresden (SDD) double zeta basis (12s11p9d8f)/[5s5p4d3f] with a small core (28 electron) effective core potential on Sm[113] and the def2-QZVPPD basis on C and O, including zero point energy corrections. These calculations reproduce the energies of the

reactants, products, and the $OSm^+(CO)$ and $Sm^+(CO_2)$ intermediates. In addition, they show that formation of a strong $SmO^+$ bond requires at least two electrons in the valence shell of Sm (non 4f).[114] The lowest energy state of $Sm^+$ that meets this requirement is a state having a $4f^5 5d^1 6s^1$ configuration, 2.35 eV above the GS $^8F_{1/2}(4f^6 6s^1)$.[114] The observed barrier is the result of the diabatic curve crossing between the surfaces evolving from these two states, Fig. 1. The calculated crossing point (CP, in reality a seam between these multidimensional surfaces) agrees well with the measured barrier height. Thus, the efficiency of activating $CO_2$ by $Sm^+$ is limited by this curve crossing, namely there is an orbital diabaticity that must be overcome for exchange of the 4f and 5d electrons.

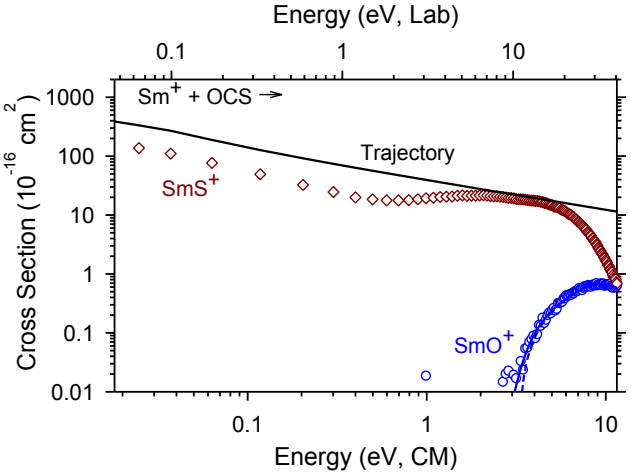


**Fig. 2.** Cross sections for reaction between $Sm^+$ and OCS as a function of energy in the center-of-mass (lower x-axis) and laboratory (upper x-axis) frames. The solid black line shows the collision cross section calculated using the trajectory model. The dashed blue line shows the model cross section, and the solid blue line is this model convoluted over the experimental energy distributions.

This issue was further explored by examining the isovalent reaction of $Sm^+$ with OCS, in a collaborative effort with the AFRL lab.[8] Both SIFT and GIBMS results find formation of only $SmS^+$ at thermal energies (with comparable efficiencies near 30%). Here, formation of $SmO^+ + CS$ is endothermic (by 1.16 ± 0.08 eV), but the threshold for formation of these products was measured to be 1.6 ± 0.3 eV above the thermodynamic threshold (Fig. 2), consistent with the behavior observed in $CO_2$ system. Our theoretical analysis shows that this excess barrier has the same origins as that for $CO_2$, again involving a crossing between the sextet surfaces originating from different 4f orbital occupations. Interestingly, this crossing seam does *not* inhibit the formation of the $SmS^+ + CO$ products. This reaction is exothermic by 0.23 ± 0.09 eV (as assessed in an independent study of $SmS^+$ that determined $D_0(Sm^+\text{-}S)$ as 3.37 ± 0.09 eV from four different processes[4]). Here, the theoretical PESs show that formation of the $SmS^+$ triple bond still requires the same curve crossing, but it now occurs *below* the reactant asymptote, thereby allowing more facile movement of a 4f electron into the 5d orbital. We believe that this orbital adiabaticity is enhanced by the ability of sulfur to develop radical character more easily (a consequence of the much weaker OC-S bond (3.14 eV) and the larger polarizability of S compared to O). Notably, it can be seen that the probability of forming $SmS^+$ increases beginning about 0.7 eV, Fig. 2, reacting near the collision limit[115] until past 3 eV. This increase can be attributed to formation of an $^8\Gamma$ excited state of $SmS^+$ calculated to lie 0.72 eV above the $^6\Sigma^+$ GS. Thus, this high-energy feature is *spin-conserving*, indicating that spin can remain a viable quantum number even for such heavy elements.

In our examination of the $SmS^+$ thermochemistry, we also determined BDEs for $SSm^+$–O, 3.73 ± 0.16 eV, and $OSm^+$–S, 1.38 ± 0.27 eV. Multiple theoretical methods were used to characterize the $SmS^+$ molecule, including high-level MRCI + Q and FPD (Feller-Peterson-Dixon)[116] approaches (collaboratively with Prof. Peterson). Spin-orbit coupling makes assignment of the GS difficult as there are multiple low-lying electronic states associated with different populations of the nonbonding 4f orbitals. All calculations underestimate the $SmS^+$ BDE, although

several methods come close to the experimental value. Similar discrepancies (0.23 – 0.47 eV) were obtained for SmO and $SmO^+$, whereas the advanced FPD approach quantitatively predicts the EuO BDE (where the half-filled 4f shell leads to only a single low-lying electronic state). Although these discrepancies are not yet fully understood, they clearly indicate a need for further theoretical advances necessitated by the benchmark experimental thermodynamics provided by our work.

Finally, we also examined the reactions of $Sm^+$ with $H_2$, $D_2$, and HD.[11] These reactions provide the simplest example of sigma bond activation and can be readily compared with similar GIBMS results available for most transition metals and many main group elements. This study measured $D_0(SmH^+)$ as 2.03 ± 0.06 eV and the $SmH^+/SmD^+$ branching ratio in the HD reaction indicates that the reaction proceeds via a direct mechanism with short-lived intermediates. This result is consistent with the $6s^14f^6$ orbital occupation of GS $Sm^+(^8F)$, as also shown by extensive theoretical computations of the $SmH_2^+$ PES. These calculations generally overestimate the $SmH^+$ BDE, although spin-orbit corrections improve the agreement considerably and CCSD(T)/CBS (complete basis set extrapolation) reproduce the experimental BDE well. Periodic trends across the lanthanide series and insights into the role of the electronic configurations on hydride bond strength and reactivity with $H_2$ were also discussed.

**Reactions involving gadolinium and neodymium. Chemi-ionization thermochemistry.** Gadolinium (Gd) and neodymium (Nd) were two of the lanthanides (along with lanthanum) suggested by Bernhardt et al. as likely candidates for further chemical release experiments.[19] As for the Sm system, we examined several reactions in order to ascertain the thermochemistry of reaction 1 with Gd and Nd.[3, 12] Both $Gd^+$ and $Nd^+$ react in barrierless exothermic reactions with $O_2$ and $CO_2$ and endothermically yield $MO^+$ (as well as $MC^+$) in reactions of CO. Additional information is obtained from the CID reactions of $MO^+$ with Xe, $O_2$, and CO as well as the reverse reaction, $MO^+ + CO \rightarrow M^+ + CO_2$. In the case of Gd, five $GdO^+$ BDEs (7.46 ± 0.26, 7.57 ± 0.34, 7.83 ± 0.19, 7.75 ± 0.17, and 7.61 ± 0.27 eV, respectively) were combined as a weighted average to yield a final value of $D_0(Gd^+\text{-}O)$ = 7.69 ± 0.10 eV (along with BDEs for $GdC^+$ and $GdCO^+$). Theoretical analyses of $GdO^+$, $GdC^+$, and $GdCO^+$ were also conducted. Our $GdO^+$ BDE agrees with literature values ranging from 7.0 ± 1.2 eV to 7.81 ± 0.13 eV and with a "best" literature value of 7.76 ± 0.16 eV.[3] Combined with IE(Gd) and $D_0$(GdO), we obtained a refined IE(GdO) value of 5.82 ± 0.16 eV, much lower than literature values of 6.5 ± 0.8 and 6.7 ± 0.5 eV.[117-118]

Experimental results for reactions of $Nd^+$ and $NdO^+$ are shown in Fig. 3[12] and are illustrative for all three metal systems (Sm, Gd, and Nd). (These figures also illustrate the wide range of kinetic energies and extensive dynamic range available to our apparatus.) Here, BDEs of 7.22 ± 0.14, 7.24 ± 0.16, 7.31 ± 0.10, 7.37 ± 0.32, and 7.27 ± 0.27 eV, respectively, were obtained and averaged to yield a final $D_0(Nd^+\text{-}O)$ = 7.28 ± 0.10 eV (along with BDEs for $NdC^+$, $NdCO^+$, and $NdO_2^+$). Again, theoretical analyses of the binding and BDEs of $NdO^+$, $NdC^+$, $NdCO^+$, and $NdO_2^+$ were conducted. Our $NdO^+$ BDE is well below literature values, which range from 7.72 ± 0.3 eV to 7.84 ± 0.19 eV, but these are flawed by having been calculated using IE(NdO) = 4.97 ± 0.10 eV from Ackermann, Rauh, and Thorn.[104] In parallel with our study, VanGundy, Persinger, and Heaven remeasured IE(NdO) as 5.5083 ± 0.0002 eV,[119] which they combined with our value of $D_0(NdO^+)$ and IE(Nd) to obtain $D_0$(NdO) = 7.26 ± 0.10 eV, comparable to literature values ranging from 7.16 ± 0.06 up to 7.48 ± 0.2 eV and a "best" value of 7.23 ± 0.08 eV.[12]

Combined with IE(M), our values for $D_0(MO^+)$ indicate that the CI reaction 1 is exothermic by 1.54 ± 0.10 eV for Gd and 1.76 ±0.10 eV for Nd, making these two metals viable candidates for efficient CI reactions. This conclusion is consistent with Fite's original measurements as well as a recent AFRL reevaluation of the CI reaction with Nd.[112]

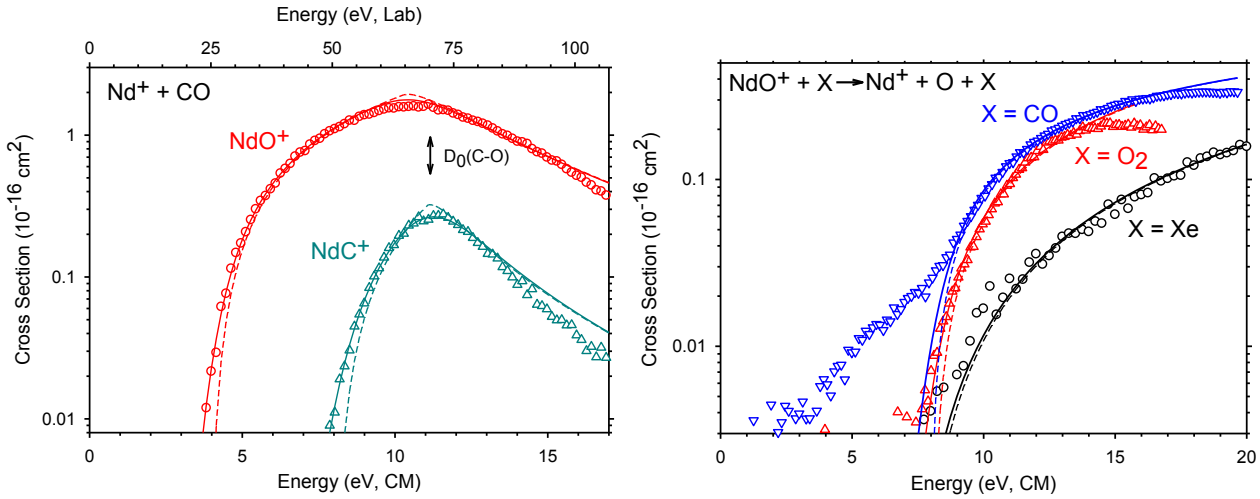


**Fig. 3.** Cross sections for the reaction of $Nd^+$ with CO (part a) and $NdO^+$ with Xe, $O_2$, and CO (part b) as functions of kinetic energy in the center-of-mass (lower x-axis) and laboratory (upper x-axis, part a) frames. Solid (dashed) lines are models of the cross section including (excluding) convolution over the kinetic and internal energy distributions of the reactants. In part a, the arrow indicates the bond energy of the CO reactant. In part b, the low energy tail in the X = CO cross section is associated with $Nd^+ + CO_2$ formation.

**Reactions involving gadolinium and neodymium. Potential energy surfaces and thermochemistry.** As for Sm, the $Gd^+ + CO_2$ PES was explored both experimentally and computationally. Unlike $Sm^+$, the $Gd^+ + CO_2 \rightarrow GdO^+ + CO$ reaction is barrierless, exothermic, and efficient (77 ± 15% of the collision limit at thermal energies) and the reverse reaction exhibits a threshold at the thermodynamic limit. CID experiments of $Gd^+(OCO)$ and $OGd^+(CO)$ intermediates yield BDEs of 0.38 ± 0.05 and 0.57 ± 0.05 eV, respectively, although comparison to theory identifies the former as an electronically excited state. Computations also show that GS $Gd^+$ ($^{10}D$) + $CO_2$ ($^1\Sigma_g^+$) reactants form GS $GdO^+$ ($^8\Sigma^-$) + CO ($^1\Sigma^+$) products in a formally spin-forbidden process, but octet and dectet surfaces have a small energy gap in the entrance channel, such that they can readily mix. Beginning near 3.3 eV, the measured $GdO^+$ + CO cross section exhibits a distinct increase, assigned to electronically excited $GdO^+$ ($^{10}\Pi$, $^{10}\Sigma^-$) products in a diabatic and spin-allowed process. Notably, the very different behavior of $Sm^+$ and $Gd^+$ reacting with $CO_2$ has the same explanation, namely, efficient reaction to form $MO^+$ + CO requires two non-4f valence electrons, but GS $Gd^+$ ($^{10}D$, $6s^15d^14f^7$) satisfies this condition. Thus, unlike the 2.35 eV excitation required for $Sm^+$, the promotion energy for $Gd^+$ is zero.

The PES for the $GdO_2^+$ system was also examined more thoroughly.[5] Fig. 4 shows that this could be accomplished, in part, because CID experiments indicated the presence of two $GdO_2^+$ ion populations, assigned to a weakly bound oxygen molecule adduct, $Gd^+(O_2)$, and an inserted Gd dioxide cation, $OGdO^+$. Source conditions could alter the relative populations of these two species. $D_0(Gd^+–O_2)$ and $D_0(OGd^+–O)$ were measured as 0.75 ± 0.11 eV ($Gd^+$ cross section, Fig. 4) and 2.86 ± 0.08 eV (high energy feature of $GdO^+$ cross section, Fig. 4), respectively. The barrier separating the two intermediates, 0.31 ± 0.07 eV relative to $Gd^+(O_2)$ (low energy feature in $GdO^+$ cross section, Fig. 4) was also extracted. These data allow a detailed *experimental* characterization of the $GdO_2^+$ PES, which was then favorably compared with theoretical calculations.

Studies of the reaction of $Gd^+$ with $H_2$, $D_2$, and HD yielded a $GdH^+$ BDE of 2.18 ± 0.07 eV, which is generally overestimated by theory.[10] The HD branching ratio suggests that $Gd^+$ reacts with dihydrogen primarily via a statistical insertion mechanism with contributions from direct mechanisms. Compared to $Sm^+$, the mechanism changes because the two non-4f valence electrons

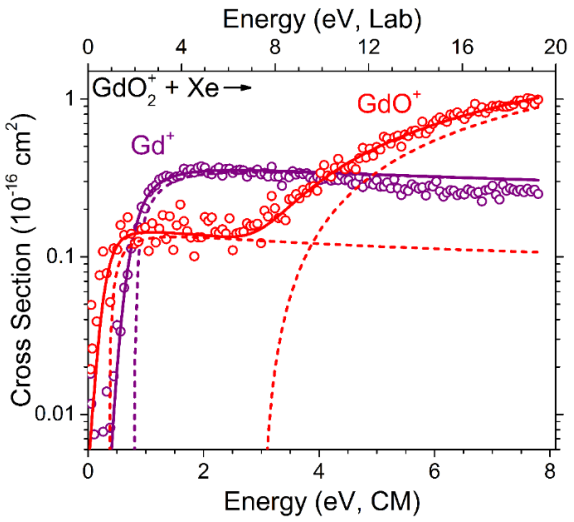


**Fig. 4.** Product ion cross sections from CID of $GdO_2^+$ as a function of center-of-mass (bottom *x*-axis) and laboratory (top *x*-axis) frame kinetic energy. Optimized models for the $GdO^+$ and $Gd^+$ cross sections are indicated by the solid (dashed) lines with (without) convolution with the reactant kinetic and internal energy distributions.

available to GS $Gd^+$ ($^{10}D$) allow facile formation of a strongly bound $GdH_2^+$ intermediate. Theoretical PESs for $GdH_2^+$ are consistent with the availability of both statistical and direct reaction pathways. The reactivity and hydride BDE for $Gd^+$ was compared with previous results for the group 3 metal cations, $Sc^+$ and $Y^+$, and the lanthanides, $La^+$ and $Lu^+$, and periodic trends were discussed.

**Auxiliary studies.** In addition to our studies of lanthanide chemistry and thermodynamics, we also engaged in several studies at the behest of the plasma chemistry group at AFRL. In one of these, the AFRL group directly measured rate constants for the CI reactions 1 of La (lanthanum), Pr (praseodymium), Tb (terbium), and Ho (holmium)[2] for comparison to previous work examining Sm and Nd.[112] As for Nd, La and Tb reacted near the calculated collision limit, consistent with all three processes being strongly exothermic. In contrast, reactions of Pr and Ho were only about 40% efficient throughout the temperature range examined (200-450 K), which is consistent with the near thermoneutral reaction of Ho, but inconsistent with the strongly exothermic reaction expected for Pr. The PI assisted in attempting to explain these results more comprehensively (and thereby make better predictions for all lanthanides) but an explanation for the inefficiency of the Pr reaction remained elusive. The CI reaction forming $LaO^+ + N_2 + e^-$ from La + $N_2O$ was also measured and found to be much slower than the competing process forming LaO + $N_2$ (by a factor of ~100), in contrast to literature data.[110]

Our groups also combined forces to examine reactions of iron carbonyl cations, $Fe^+(CO)_n$ where n = 1 and 2, with $O_2$,[7] of interest as a model system for removal of CO by oxidation to $CO_2$ (e.g., in treatment of engine exhaust), which generally requires expensive metal catalysts and intensive temperature and pressure conditions.[120-124] (Notably, this rationale for study is also appropriate for our studies of the $MO^+$ + CO chemistry outlined above.) Rate constants from 300 – 600 K were measured, with $Fe^+(CO)$ oxidizing the CO ligand to $CO_2$ in an efficient, exothermic process. Thus, O-O bond cleavage and O-CO bond formation occur facilely at a single non-noble metal atom. In contrast, $Fe^+(CO)_2$ is unreactive with $O_2$. Further details of the reaction with the monocarbonyl were revealed by GIBMS studies, which showed that the efficiency of the reaction declines as $E^{-1/2}$, consistent with a curve crossing between surfaces of different spin.[43] This conclusion was corroborated by theoretical calculations showing that the reaction is an example of two-state reactivity requiring a crossing from sextet to quartet spin surfaces. Calculations also show that the key difference between $Fe^+(CO)_n$ (n = 1 and 2) reactants is a deeper well associated with the $(O_2)Fe^+(CO)_n$ intermediate for n = 1, which then allows the transition state leading to the dioxide, $OFeO^+(CO)_n$ to lie below the reactant energy. The curve crossing lies past the dioxide and allows a low-energy pathway for O-CO coupling leading to $CO_2$. Observation of endothermic formation of $FeO_2^+$ + CO in the n = 1 reaction helped confirm details of the calculated PES.

Finally, our groups along with the theoretician, Prof. Hua Guo at U. New Mexico,

reexamined the reaction of gold dimer cations, $Au_2^+$, with methane,[14] which had been reported to yield ethene in a "catalytic" process at 300 K and below.[125-127] This reaction is of potential industrial utility as a means of activating the inert methane molecule to a more valuable and easily used chemical. AFRL SIFT studies saw no evidence for formation of $Au_2^+(C_2H_4)$ at *m/z* 422, observing only association reactions. This result is consistent with the known thermodynamics as transformation of 2 $CH_4$ molecules to $C_2H_4$ + 2 $H_2$ is endothermic by 2.088 eV. Thus, an equilibrium distribution at 300 K favors reactants by *30 orders of magnitude*. Our GIBMS studies were generally consistent with the SIFT studies but did observe an inefficient, exothermic reaction of $Au_2^+(CH_4) + CH_4$ forming the purported *m/z* 422 product (where the extent of product formation was very sensitive to source conditions). Additional work suggested that this product is actually $Au_2^+(CO)$ formed in the reaction of $CH_4$ with $Au_2O^+$ (isobaric with the methane adduct) and that formation of $Au_2O^+$ requires generation of electronically excited $Au^+$ or $Au_2^+$, which might have sufficient energy to drive the reaction converting methane to ethene. Notably, this publication was recognized as a "2019 Catalysis Science & Technology HOT Article". Coupled with this study, we measured the $Au_2^+$ bond energy for the first time (2.20 ± 0.21 eV), and coupled that with calculations of this species in collaboration with Prof. Guo. This work was published as a "Featured Article" in *J. Chem. Phys*.[13]

**Appendix I. Bibliography and References Cited**

(first 14 publications are for AFOSR sponsored research)


1. Cox, R. M.; Kim, J.; Armentrout, P. B.; Bartlett, J.; VanGundy, R. A.; Heaven, M. C.; Ard, S. G.; Melko, J. J.; Shuman, N. S.; Viggiano, A. A. Evaluation of the Exothermicity of the Chemi-ionization Reaction Sm + O → $SmO^+ + e^-$. *J. Chem. Phys.* **2015,** *142*, 134307.
2. Ard, S. G.; Shuman, N. S.; Martinez, O.; Armentrout, P. B.; Viggiano, A. A. Chemi-ionization reactions of La, Pr, Tb, and Ho with atomic O and La with $N_2O$ from 200 - 450 K. *J. Chem. Phys.* **2016,** *145*, 084302.
3. Demireva, M.; Kim, J.; Armentrout, P. B. Gadolinium (Gd) Oxide, Carbide, and Carbonyl Cation Bond Energies and Evaluation of the Gd + O → $GdO^+ + e^-$ Chemi-Ionization Reaction Enthalpy. *J. Phys. Chem. A* **2016,** *120*, 8550-8563.
4. Armentrout, P. B.; Demireva, M.; Peterson, K. A. Guided Ion Beam and Theoretical Studies of the Bond Energy of $SmS^+$. *J. Chem. Phys.* **2017,** *147*, 214307.
5. Demireva, M.; Armentrout, P. B. Gadolinium Cation ($Gd^+$) Reaction with $O_2$: Potential Energy Surface Mapped Experimentally and with Theory. *J. Chem. Phys.* **2017,** *146*, 174302.
6. Armentrout, P. B.; Cox, R. M. Potential Energy Surface for Reaction of $Sm^+ + CO_2$ → $SmO^+ + CO$: Guided Ion Beam and Theoretical Studies. *Phys. Chem. Chem. Phys.* **2017,** *19*, 11075-11088.
7. Ard, S. G.; Martinez, O.; Brown, S. A.; Sawyer, J. C.; Armentrout, P. B.; Viggiano, A. A.; Shuman, N. S. Reactivity of $^4Fe^+(CO)_{n=0-2} + O_2$: Oxidation of CO by $O_2$ at an isolated metal atom. *Phys. Chem. Chem. Phys.* **2017,** *19*, 8768-8777.
8. Armentrout, P. B.; Cox, R. M.; Sweeny, B. C.; Ard, S. G.; Shuman, N. S.; Viggiano, A. A. Lanthanides as Catalysts: Guided Ion Beam and Theoretical Studies of $Sm^+ + COS$. *J. Phys. Chem. A* **2018,** *122*, 737-749.
9. Demireva, M.; Armentrout, P. B. Activation of $CO_2$ by Gadolinium Cation ($Gd^+$): Energetics and Mechanism from Experiment and Theory. *Top. Catal.* **2018,** *61*, 3-19.

10. Demireva, M.; Armentrout, P. B. Activation of $H_2$ by Gadolinium Cation ($Gd^+$): Bond Energy of $GdH^+$ and Mechanistic Insights from Guided Ion Beam and Theoretical Studies. *J. Phys. Chem. A* **2018,** *122*, 750-761.
11. Demireva, M.; Armentrout, P. B. Samarium Cation ($Sm^+$) Reactions with $H_2$, $D_2$, and HD: $SmH^+$ Bond Energy and Mechanistic Insights from Guided Ion Beam and Theoretical Studies *J. Chem. Phys.* **2018,** *149*, 164304.
12. Ghiassee, M.; Kim, J.; Armentrout, P. B. Evaluation of the exothermicity of the chemi-ionization reaction $Nd + O \rightarrow NdO^+ + e^-$ and neodymium oxide, carbide, dioxide, and carbonyl cation bond energies. *J. Chem. Phys.* **2019,** *150*, 144309.
13. Owen, C. J.; Keyes, N. R.; Xie, C.; Guo, H.; Armentrout, P. B. Bond Dissociation Energy of $Au_2^+$: A Guided Ion Beam and Theoretical Investigation. *J. Chem. Phys.* **2019,** *150*, 174305.
14. Shuman, N. S.; Ard, S. G.; Sweeny, B. C.; Pan, H.; Viggiano, A. A.; Keyes, N. R.; Guo, H.; Owen, C. J.; Armentrout, P. B. $Au_2^+$ Cannot Catalyze Conversion of Methane to Ethene at Low Temperature. *Catal. Sci. Tech.* **2019,** *9*, 2767-2780.
15. Caton, R. G.; Pedersen, T. R.; Groves, K. M.; Hines, J.; Cannon, P. S.; Jackson-Booth, N.; Parris, R. T.; Holmes, J. M.; Su, Y.-J.; Mishin, E. V., et al. Artificial Ionospheric Modification: The Metal Oxide Space Cloud Experiment. *Radio Science* **2017,** *52*, 539-558.
16. Schofield, K. An Overlooked Series of Gas Phase Diatomic Metal Oxide Ions That Are Long-lived. *J. Phys. Chem. A* **2006,** *110*, 6938-6947.
17. Lide, D. R., *CRC Handbook of Chemistry and Physics*. CRC Press: Boca Raton, 2002; Vol. 83.
18. Zhang, Y.; Evans, J. R. G.; Yang, S. Corrected Values for Boiling Points and Enthalpies of Vaporization of Elements in Handbooks. *J. Chem. Eng. Data* **2011,** *56*, 328-337.
19. Bernhardt, P. A.; Siefring, C. L.; Briczinski, S. J.; Viggiano, A.; Caton, R. G.; Pedersen, T. R.; Holmes, J. M.; Ard, S.; Shuman, N.; Groves, K. M. A Physics-based Model for the Ionization of Samarium by the MOSC Chemical Releases in the Upper Atmosphere. *Radio Science* **2017,** *52*, 559-577.
20. Ervin, K. M.; Armentrout, P. B. Translational Energy Dependence of $Ar^+ + XY \rightarrow ArX^+ + Y$ ($XY = H_2$, $D_2$, HD) from Thermal to 30 eV c.m. *J. Chem. Phys.* **1985,** *83*, 166-189.
21. Armentrout, P. B. The Kinetic Energy Dependence of Ion-Molecule Reactions: Guided Ion Beams and Threshold Measurements. *Int. J. Mass Spectrom.* **2000,** *200*, 219-241.
22. Armentrout, P. B. Not Just a Structural Tool: The Use of Guided Ion Beam Tandem Mass Spectrometry to Determine Thermochemistry. *J. Am. Soc. Mass Spectrom.* **2002,** *13*, 419-434.
23. Armentrout, P. B., Thermochemical Measurements by Guided Ion Beam Mass Spectrometry. In *Adv. Gas Phase Ion Chem.*, Adams, N.; Babcock, L. M., Eds. JAI Press: Greenwich, Connecticut, 1992; Vol. 1, pp 83-119.
24. Armentrout, P. B.; Simons, J. Understanding Heterolytic Bond Cleavage. *J. Am. Chem. Soc.* **1992,** *114*, 8627-8633.
25. Schultz, R. H.; Armentrout, P. B. Reactions of $N_4^+$ with Rare Gases from Thermal to 10 eV c.m.: Collision-Induced Dissociation, Charge Transfer, and Ligand Exchange. *Int. J. Mass Spectrom. Ion Processes* **1991,** *107*, 29-48.
26. Haynes, C. L.; Armentrout, P. B.; Perry, J. K.; Goddard, W. A., III Experimental and Theoretical Studies of $Co(CH_4)_x^+$ with $x = 1 - 4$. *J. Phys. Chem.* **1995,** *99*, 6340-6346.
27. Tjelta, B. L.; Armentrout, P. B. Gas-Phase Metal Ion Ligation: Collision-Induced Dissociation of $Fe(N_2)_x^+$ ($x = 1 - 5$) and $Fe(CH_2O)_x^+$ ($x = 1 - 4$). *J. Phys. Chem. A* **1997,** *101*, 2064-2073.

28. Walter, D.; Sievers, M. R.; Armentrout, P. B. Alkali Ion Carbonyls: Sequential Bond Energies of $Li^+(CO)_x$ ($x$ = 1 - 3), $Na^+(CO)_x$ ($x$ = 1, 2), and $K^+(CO)$. *Int. J. Mass Spectrom.* **1998,** *173*, 93-106.
29. Andersen, A.; Muntean, F.; Walter, D.; Rue, C.; Armentrout, P. B. Collision-Induced Dissociation and Theoretical Studies of $Mg^+$ Complexes with CO, $CO_2$, $NH_3$, $CH_4$, $CH_3OH$, and $C_6H_6$. *J. Phys. Chem. A* **2000,** *104*, 692-705.
30. Tjelta, B. L.; Walter, D.; Armentrout, P. B. Determination of Weak $Fe^+$-L Bond Energies (L = Ar, Kr, Xe, $N_2$, $CO_2$) by Ligand Exchange Reactions and Collision-Induced Dissociation. *Int. J. Mass Spectrom.* **2001,** *204*, 7-21.
31. Armentrout, P. B.; Kickel, B. L., Gas-Phase Thermochemistry of Transition Metal Ligand Systems: Reassessment of Values and Periodic Trends. In *Organometallic Ion Chemistry*, Freiser, B. S., Ed. Kluwer: Dordrecht, 1996; pp 1-45.
32. Armentrout, P. B., Gas Phase Organometallic Chemistry. In *Topics in Organometallic Chemistry*, Brown, J. M.; Hofmann, P., Eds. Springer-Verlag: Berlin, 1999; Vol. 4, pp 1-45.
33. Cox, R. M.; Armentrout, P. B.; de Jong, W. A. Activation of $CH_4$ by $Th^+$ as Studied by Guided Ion Beam Mass Spectrometry and Quantum Chemistry. *Inorg. Chem.* **2015,** *54*, 3584-3599.
34. Cox, R. M.; Citir, M.; Armentrout, P. B.; Battey, S. R.; Peterson, K. A. Bond Energies of $ThO^+$ and $ThC^+$: A Guided Ion Beam and Quantum Chemical Investigation of the Reactions of Thorium Cation with $O_2$ and CO. *J. Chem. Phys.* **2016,** *144*, 184309.
35. Cox, R. M.; Armentrout, P. B.; de Jong, W. A. Reactions of $Th^+ + H_2$, $D_2$, and HD Studied by Guided Ion Beam Tandem Mass Spectrometry and Quantum Chemical Calculations. *J. Phys. Chem. B* **2016,** *120*, 1601-1614.
36. Cox, R. M.; Armentrout, P. B. Activation of Water by Thorium Cation: A Guided Ion Beam and Quantum Chemical Study. *J. Am. Soc. Mass Spectrom.* **2019,** *30*, 1835-1849.
37. Kafle, A.; Armentrout, P. B. Mechanism and Energetics of the Hydrolysis of $Th^+$ To Form $Th(OD)_3^+$: Guided Ion Beam and Theoretical Studies of $ThO^+$, $ThO_2^+$, and $OThOD^+$ Reacting with $D_2O$. *J. Phys. Chem. A* **2019,** *123*, 5893-5905.
38. Cox, R. M.; Kafle, A.; Armentrout, P. B.; Peterson, K. A. Bond Energy of $ThN^+$: A Guided Ion Beam and Quantum Chemical Investigation of the Reactions of Thorium Cation with $N_2$ and NO. *J. Chem. Phys.* **2019,** *151*, 034304.
39. Kickel, B. L.; Armentrout, P. B. Guided Ion Beam Studies of the Reactions of $Mn^+$, $Cu^+$, and $Zn^+$ with Silane. $M^+$-$SiH_x$ ($x$ = 0 - 3) Bond Energies. *J. Phys. Chem* **1995,** *99*, 2024-2032.
40. Chen, Y.-M.; Armentrout, P. B. Kinetic Energy Dependence of the Reactions of $Ru^+$, $Rh^+$, $Pd^+$, and $Ag^+$ with $O_2$. *J. Chem. Phys.* **1995,** *103*, 618-625.
41. Taylor, W. S.; Spicer, E. M.; Barnas, D. F. Metastable Metal Ion Production in Sputtering dc Glow Discharge Plasmas: Characterization by Electronic State Chromatography. *J. Phys. Chem. A* **1999,** *103*, 643-650.
42. Rodgers, M. T.; Walker, B.; Armentrout, P. B. Reactions of $Cu^+(^1S$ and $^3D)$ with $O_2$, CO, $CO_2$, NO, $N_2O$, and $NO_2$ Studied by Guided Ion Beam Mass Spectrometry. *Int. J. Mass Spectrom.* **1999,** *182-183*, 99-120.
43. Rue, C.; Armentrout, P. B.; Kretzschmar, I.; Schröder, D.; Harvey, J. N.; Schwarz, H. Kinetic-energy Dependence of Competitive Spin-allowed and Spin-forbidden Reactions: $V^+ + CS_2$. *J. Chem. Phys.* **1999,** *110*, 7858-7870.
44. Zhang, X.-G.; Armentrout, P. B. Activation of $O_2$, CO, and $CO_2$ by $Pt^+$: The Thermochemistry of $PtO^+$. *J. Phys. Chem. A* **2003,** *107*, 8904-8914.

45. Armentrout, M. M.; Li, F.-X.; Armentrout, P. B. Is Spin Conserved in Heavy Metal Systems? Experimental and Theoretical Studies of the Reaction of $Re^+$ with Methane. *J. Phys. Chem. A* **2004,** *108*, 9660-9672.
46. Li, F.-X.; Armentrout, P. B. Activation of Methane by Gold Cations: Guided Ion Beam and Theoretical Studies. *J. Chem. Phys.* **2006,** *125*, 133114
47. Li, F.-X.; Gorham, K.; Armentrout, P. B. Oxidation of Atomic Gold Ions: Thermochemistry for the Activation of $O_2$ and $N_2O$ by $Au^+$ ($^1S_0$ and $^3D$). *J. Phys. Chem. A* **2010,** *114*, 11043–11052
48. Kickel, B. L.; Armentrout, P. B. Guided Ion Beam Studies of the Reactions of Group 3 Metal Ions ($Sc^+$, $Y^+$, $La^+$, and $Lu^+$) with Silane. Electronic State Effects, Comparison to Reactions with Methane, and $M^+$-$SiH_x$ (x = 0 - 3) Bond Energies. *J. Am. Chem. Soc.* **1995,** *117*, 4057-4070.
49. Clemmer, D. E.; Chen, Y.-M.; Khan, F. A.; Armentrout, P. B. State-Specific Reactions of $Fe^+(a^6D, a^4F)$ with $D_2O$ and Reactions of $FeO^+$ with $D_2$. *J. Phys. Chem.* **1994,** *98*, 6522-6529.
50. Haynes, C. L.; Armentrout, P. B. Thermochemistry and Structures of $CoC_3H_6^+$: Metallacycle and Metal-Alkene Isomers. *Organomet.* **1994,** *13*, 3480-3490.
51. Kickel, B. L.; Armentrout, P. B. Reactions of $Fe^+$, $Co^+$ and $Ni^+$ with Silane. Electronic State Effects and $M^+$-$SiH_x$ ($x$ = 0 - 3) Bond Energies. *J. Am. Chem. Soc.* **1995,** *117*, 764-773.
52. Chen, Y.-M.; Elkind, J. L.; Armentrout, P. B. Reactions of $Ru^+$, $Rh^+$, $Pd^+$, and $Ag^+$ with $H_2$, HD and $D_2$. *J. Phys. Chem.* **1995,** *99*, 10438-10445.
53. Sievers, M. R.; Chen, Y.-M.; Elkind, J. L.; Armentrout, P. B. Reactions of $Y^+$, $Zr^+$, $Nb^+$, and $Mo^+$ with $H_2$, HD, and $D_2$. *J. Phys. Chem.* **1996,** *100*, 54-62.
54. Walter, D.; Armentrout, P. B. Sequential Bond Dissociation Energies of $M^+(NH_3)_x$ ($x$ = 1 - 4) for M = Ti - Cu. *J. Am. Chem. Soc.* **1998,** *120*, 3176-3187.
55. Armentrout, P. B.; Rodgers, M. T. An Absolute Sodium Cation Affinity Scale: Threshold Collision-Induced Dissociation Experiments and ab Initio Theory. *J. Phys. Chem. A* **2000,** *104*, 2238-2247.
56. Rodgers, M. T.; Armentrout, P. B. Noncovalent Metal-Ligand Bond Energies as Studied by Threshold Collision-Induced Dissociation. *Mass Spectrom. Rev.* **2000,** *19*, 215-247.
57. Gerlich, D. Inhomogeneous rf Fields: A Versatile Tool for the Study of Processes with Slow Ions. *Adv. Chem. Phys.* **1992,** *82*, 1-176.
58. Muntean, F.; Armentrout, P. B. Guided Ion Beam Study of Collision-Induced Dissociation Dynamics: Integral and Differential Cross Sections. *J. Chem. Phys.* **2001,** *115*, 1213-1228.
59. Daly, N. R. Scintillation Type Mass Spectrometer Ion Detector. *Rev. Sci. Instrum.* **1960,** *31*, 264-267.
60. Burley, J. D.; Ervin, K. M.; Armentrout, P. B. Translational Energy Dependence of $O^+(^4S)$ + $H_2(D_2, HD) \rightarrow OH^+(OD^+)$ + H(D) from Thermal to 30 eV c.m. *Int. J. Mass Spectrom. Ion Processes* **1987,** *80*, 153-175.
61. Gioumousis, G.; Stevenson, D. P. Reactions of Gaseous Molecule Ions with Gaseous Molecules. V. Theory. *J. Chem. Phys.* **1958,** *29*, 294-299.
62. Robinson, P. J.; Holbrook, K. A., *Unimolecular Reactions*. Wiley Interscience: New York, 1972.
63. Gilbert, R. G.; Smith, S. C., *Theory of Unimolecular and Recombination Reactions*. Blackwell Scientific: London, 1990.
64. Schultz, R. H.; Crellin, K. C.; Armentrout, P. B. Sequential Bond Energies of $Fe(CO)_x^+$ ($x$ = 1 - 5): Systematic Effects on Collision-Induced Dissociation Measurements. *J. Am. Chem. Soc.* **1991,** *113*, 8590-8601.

65. Chantry, P. J. Doppler Broadening in Beam Experiments. *J. Chem. Phys.* **1971,** *55*, 2746-2759.
66. Lifshitz, C.; Wu, R. L. C.; Tiernan, T. O.; Terwilliger, D. T. Negative Ion-molecule Reactions of Ozone and Their Implications on the Thermochemistry of $O_3^-$. *J. Chem. Phys.* **1978,** *68*, 247-260.
67. Khan, F. A.; Clemmer, D. E.; Schultz, R. H.; Armentrout, P. B. Sequential Bond Energies of $Cr(CO)_x^+$, $x$ = 1 - 6. *J. Phys. Chem.* **1993,** *97*, 7978-7987.
68. Rodgers, M. T.; Ervin, K. M.; Armentrout, P. B. Statistical Modeling of Collision-Induced Dissociation Thresholds. *J. Chem. Phys.* **1997,** *106*, 4499-4508.
69. Rodgers, M. T.; Armentrout, P. B. Statistical Modeling of Competitive Threshold Collision-Induced Dissociation. *J. Chem. Phys.* **1998,** *109*, 1787-1800.
70. Amicangelo, J. C.; Armentrout, P. B. Relative and Absolute Bond Dissociation Energies of Sodium Cation Complexes Determined Using Competitive Collision-Induced Dissociation Experiments. *Int. J. Mass Spectrom.* **2001,** *212*, 301-325.
71. Muntean, F.; Armentrout, P. B. Modeling Kinetic Shifts for Tight Transition States in Threshold Collision-Induced Dissociation. Case Study: Phenol Cation. *J. Phys. Chem. B* **2002,** *106*, 8117-8124.
72. Muntean, F.; Armentrout, P. B. Modeling kinetic shifts and competition in threshold collision-induced dissociation. Case study: *n*-butylbenzene cation dissociation. *J. Phys. Chem. A* **2003,** *107*, 7413-7422.
73. Muntean, F.; Heumann, L.; Armentrout, P. B. Modeling kinetic shifts in threshold collision-induced dissociation. Case study: dichlorobenzene cation dissociation. *J. Chem. Phys.* **2002,** *116*, 5593-5602.
74. Koizumi, H.; Muntean, F.; Armentrout, P. B. Reaction of $Cu^+$ with Dimethoxyethane: Competition between Association and Multiple Dissociation Channels. *J. Chem. Phys.* **2004,** *120*, 756-766.
75. Koizumi, H.; Armentrout, P. B. The Kinetic Energy Dependence of Association Reactions. A New Thermokinetic Method for Large Systems. *J. Chem. Phys.* **2003,** *119*, 12819-12829.
76. Amicangelo, J. C.; Armentrout, P. B. Ligand Exchange Reactions of Sodium Cation Complexes Examined Using Guided Ion Beam Mass Spectrometry: Relative and Absolute Dissociation Free Energies and Entropies. *J. Phys. Chem. A* **2004,** *108*, 10698-10713.
77. Armentrout, P. B. Statistical modeling of sequential collision-induced dissociation. *J. Chem. Phys.* **2007,** *126*, 234302.
78. Hinton, C. S.; Citir, M.; Armentrout, P. B. Guided Ion-Beam and Theoretical Studies of the Reaction of $Os^+$ ($^6D$) with $O_2$: Adiabatic and Nonadiabatic Behavior. *Int. J. Mass Spectrom.* **2013,** *354-355*, 87-98.
79. Hinton, C. S.; Armentrout, P. B. Guided Ion Beam and Theoretical Study of the Reactions of $Hf^+$ with $H_2$, $D_2$, and HD *J. Chem. Phys.* **2010,** *133*, 124307.
80. Zhang, X.-G.; Rue, C.; Shin, S.-Y.; Armentrout, P. B. Reactions of $Ta^+$ and $W^+$ with $H_2$, $D_2$, and HD: Effect of Lanthanide Contraction and Spin-Orbit Interactions on Reactivity and Thermochemistry. *J. Chem. Phys.* **2002,** *116*, 5574-5583.
81. Zhang, X.-G.; Armentrout, P. B. Reactions of $Pt^+$ with $H_2$, $D_2$, and HD: Effect of Lanthanide Contraction on Reactivity and Thermochemistry. *J. Chem. Phys.* **2002,** *116*, 5565-5573.

82. Armentrout, P. B.; Li, F.-X. Probes of Spin-conservation in Heavy Metal Reactions: Experimental and Theoretical Studies of the Reactions of $Re^+$ with $H_2$, $D_2$, and HD. *J. Chem. Phys.* **2004,** *121*, 248-256.
83. Li, F.-X.; Zhang, X.-G.; Armentrout, P. B. Guided Ion Beam and Theoretical Study of the Reactions of $Ir^+$ with $H_2$, $D_2$, and HD. *J. Phys. Chem. A* **2005,** *109*, 8350-8357.
84. Li, F.-X.; Liu, F.; Armentrout, P. B. Guided Ion Beam and Theoretical Study of the Reactions of $Au^+$ with $H_2$, $D_2$, and HD *J. Chem. Phys.* **2011,** *134*, 024310.
85. Hinton, C. S.; Li, F.-X.; Armentrout, P. B. Reactions of $Hf^+$, $Ta^+$, and $W^+$ with $O_2$ and CO: Metal Carbide and Metal Oxide Cation Bond Energies. *Int. J. Mass Spectrom.* **2009,** *280*, 226-234.
86. Armentrout, P. B. The Bond Energy of $ReO^+$: Guided Ion-Beam and Theoretical Studies of the Reaction of $Re^+$ ($^7S$) with $O_2$. *J. Chem. Phys.* **2013,** *139*, 084305.
87. Armentrout, P. B.; Li, F.-X. The Bond Energy of $IrO^+$: Guided Ion-Beam and Theoretical Studies of the Reaction of $Ir^+$ ($^5F$) with $O_2$. *J. Phys. Chem. A* **2013,** *117*, 7754-7766.
88. Zhang, X.-G.; Armentrout, P. B. Activation of $O_2$ and $CO_2$ by $PtO^+$: The Thermochemistry of $PtO_2^+$. *J. Phys. Chem. A* **2003,** *107*, 8915-8922.
89. Parke, L. G.; Hinton, C. S.; Armentrout, P. B. Why is Hafnium So Unreactive? Experimental and Theoretical Studies of the Reaction of $Hf^+$ with Methane. *Int. J. Mass Spectrom.* **2006,** *254*, 168-182.
90. Parke, L. G.; Hinton, C. S.; Armentrout, P. B. Experimental and Theoretical Studies of the Activation of Methane by $Ta^+$ and the Bond Energies of $Ta^+$-$CH_x$ (x = 1 - 3). *J. Phys. Chem. C* **2007,** *111*, 17773-17787.
91. Armentrout, P. B.; Shin, S.; Liyanage, R. Guided-Ion Beam and Theoretical Study of the Potential Energy Surface for Activation of Methane by $W^+$ *J. Phys. Chem. A* **2006,** *110*, 1242-1260.
92. Armentrout, P. B.; Parke, L.; Hinton, C.; Citir, M. Activation of Methane by $Os^+$: Guided Ion Beam and Theoretical Studies. *ChemPlusChem* **2013,** *78*, 1157-1173.
93. Li, F.-X.; Zhang, X.-G.; Armentrout, P. B. The Most Reactive Third-row Transition Metal: Guided Ion Beam and Theoretical Studies of the Activation of Methane by $Ir^+$. *Int. J. Mass Spectrom.* **2006,** *255/256*, 279-300.
94. Zhang, X.-G.; Liyanage, R.; Armentrout, P. B. The Potential Energy Surface for Activation of Methane by $Pt^+$: A Detailed Guided-Ion Beam Study. *J. Am. Chem. Soc.* **2001,** *123*, 5563-5575.
95. Parke, L. G.; Hinton, C. S.; Armentrout, P. B. Energetics and Mechanisms of C-H Bond Activation by a Doubly-charged Metal Ion: Guided Ion Beam and Theoretical Studies of $Ta^{2+}$ + $CH_4$. *J. Phys. Chem. A* **2008,** *112*, 10469–10480.
96. Ames, L. L.; Walsh, P. N.; White, D. Rare Earths. IV. Dissociation Energies of the Gaseous Monoxides of the Rare Earths. *J. Phys. Chem.* **1967,** *71*, 2707-2718.
97. Dickson, C. R.; Zare, R. N. Beam Gas Chemiluminescent Reactions of Eu and Sm with $O_3$, $N_2O$, $NO_2$, and $F_2$. *Chem. Phys.* **1975,** *7*, 361.
98. Hildenbrand, D. L. Dissociation Energy of Samarium Monoxide and Its Relation to That of Europium Monoxide. *Chem. Phys. Lett.* **1977,** *48*, 340.
99. Brewer, L.; Rosenblatt, G. M., Dissociation Energies and Free Energy Functions of Gaseous Monoxides. In *Adv. High Temp. Chem.*, Eyring, L., Ed. Academic: New York, 1969; Vol. 2, pp 1-83.
100. Pedley, J. B.; Marshall, E. M. Thermochemical Data for Gaseous Monoxides. *J. Phys. Chem. Ref. Data* **1983,** *12*, 967-1031.

101. Chandrasekharaiah, M. S.; Gingerich, K. A., In *Handbook on the Physics and Chemistry of Rare Earths*, Gschniedner, K. A.; Jr., L. E., Eds. Elsevier: Amsterdam, 1989.
102. Lias, S. G.; Bartmess, J. E.; Liebman, J. F.; Holmes, J. L.; Levin, R. D.; Mallard, W. G. Gas-Phase Ion and Neutral Thermochemistry. *J. Phys. Chem. Ref. Data Suppl. 1* **1988,** *17*, 1.
103. Konings, R. J. M.; Benes, O.; Kovacs, A.; Manara, D.; Sedmidubsky, D.; Gorokhov, L.; Iorish, V. S.; Yungman, V.; Shenyavskaya, E.; Osina, E. The Thermodynamic Properties of the f-Elements and their Compounds. Part 2. The Lanthanide and Actinide Oxides. *J. Phys. Chem. Ref. Data* **2014,** *43*, 013101.
104. Ackermann, R. J.; Rauh, E. G.; Thorn, R. J. The thermodynamics of ionization of gaseous oxides; the first ionization potentials of the lanthanide metals and monoxides. *J. Chem. Phys.* **1976,** *65*, 1027-1031.
105. Jayasekharan, T.; Razvi, M. A. N.; Bhale, G. L. Even-parity bound and autoionizing Rydberg series of the samarium atom. *J. Phys. B: At. Mol. Opt. Phys.* **2000,** *33*, 3123-3136.
106. Martin, W. C.; Zalubas, R.; Hagan, L. Atomic Energy Levels - The Rare Earth Elements. *Natl. Stand. Ref. Data Ser., Natl. Bur. Stand. (U.S.)* **1978,** *60*, 1.
107. Sievers, M. R.; Chen, Y.-M.; Armentrout, P. B. Metal Oxide and Carbide Thermochemistry of $Y^+$, $Zr^+$, $Nb^+$, and $Mo^+$. *J. Chem. Phys.* **1996,** *105*, 6322-6333.
108. Hinton, C. S.; Citir, M.; Manard, M.; Armentrout, P. B. Collision-induced Dissociation of $MO^+$ and $MO_2^+$ (M = Ta and W): Metal Oxide and Dioxide Cation Bond Energies. *Int. J. Mass Spectrom.* **2011,** *308*, 265-274.
109. Rauh, E. G.; Ackermann, R. J. First Ionization Potentials of Some Refractory Oxide Vapors *J. Chem. Phys.* **1974,** *60*, 1396-1400.
110. Fite, W. L.; Patterson, T. A.; Siegel, M. W. *Cross Sections for Thermal Reactions Between Uranium Atoms and Atmospheric Species*; Air Force Geophysics Laboratory, Hanscom Air Force Base MA, Report No. AFGL-TR-77-0030, NTIS Access No. AD/A 038806: 1976; pp 1-88.
111. Cockett, M. C. R.; Nyulaszi, L.; Veszpremi, T.; Wright, T. G.; Dyke, J. M. A Study of Some Gas-Phase Lanthanide Plus Oxidant Chemiionization Reactions with Chemielectron Spectroscopy. *J. Electron Spectros. Relat. Phenom.* **1991,** *57*, 373-397.
112. Ard, S. G.; Shuman, N. S.; O. Martinez, J.; Brumbach, M. T.; Viggiano, A. A. Kinetics of chemi-ionization reactions of lanthanide metals (Nd, Sm) from 150 to 450 K. *J. Chem. Phys.* **2015,** *143*, 204303.
113. Dolg, M.; Stoll, H.; Preuss, H. Energy-Adjusted Ab Initio Pseudopotentials for the Rare Earth Elements. *J. Chem. Phys.* **1989,** *90*, 1730-1734.
114. Gibson, J. K. Role of Atomic Electronics in f-Element Bond Formation: Bond Energies of Lanthanide and Actinide Oxide Molecules. *J. Phys. Chem. A* **2003,** *107*, 7891-7899.
115. Su, T.; Chesnavich, W. J. Parameterization of the Ion-polar Molecule Collision Rate Constant by Trajectory Calculations. *J. Chem. Phys.* **1982,** *76*, 5183-5185.
116. Feller, D.; Peterson, K. A.; Dixon, D. A. A Survey of Factors Contributing to Accurate Theoretical Predictions of Atomization Energies and Molecular Structures. *J. Chem. Phys.* **2008,** *129* 204105.
117. Kordis, J.; Gingerich, K. A. Mass spectrometric observations of some polyatomic gaseous rare earth oxides and their atomization energies. *J. Chem. Phys.* **1977,** *66*, 483-491.
118. Murad, E.; Hildenbrand, D. L. Dissociation energies of GdO, HoO, ErO, TmO, and LuO; correlation of results for the lanthanide monoxide series. *J. Chem. Phys.* **1980,** *73*, 4005-4011.
119. VanGundy, R. A.; Persinger, T. D.; Heaven, M. C. Low energy states of $NdO^+$ probed by photoelectron spectroscopy. *J. Chem. Phys.* **2019,** *150*, 114302.

120. Alavi, A.; Hu, P. J.; Deutsch, T.; Silvestrelli, P. L.; Hutter, J. CO Oxidation on Pt(111): An Ab Initio Density Functional Theory Study. *Phys. Rev. Lett.* **1998,** *80*, 3650-3653.
121. Zambelli, T.; Barth, J. V.; Wintterlin, J.; Ertl, G. Complex Pathways in Dissociative Adsorption of Oxygen on Platinum. *Nature* **1997,** *390*, 495-497.
122. Liu, Z. P.; Hu, P.; Alavi, A. Catalytic Role of Gold in Gold-Based Catalysts: A Density Functional Theory Study on the CO Oxidation on Gold. *J. Am. Chem. Soc.* **2002,** *124*, 14770-14779.
123. Stampfl, C.; Scheffler, M. Anomalous Behavior of Ru for Catalytic Oxidation: A Theoretical Study of the Catalytic Reaction CO +1/2 $O_2$ → $CO_2$. *Phys. Rev. Lett.* **1997,** *78*, 1500-1503.
124. Kondoh, H.; Toyoshima, R.; Monya, Y.; Yoshida, M.; Mase, K.; Amemiya, K.; Mun, B. S. In Situ Analysis of Catalytically Active Pd Surfaces for CO Oxidation with Near Ambient Pressure XPS. *Catalysis Today* **2016,** *260*, 14-20.
125. Lang, S. M.; Bernhardt, T. M.; Barnett, R. N.; Landman, U. Methane Activation and Catalytic Ethylene Formation on Free $Au_2^+$. *Angew. Chem. Int. Ed.* **2010,** *49*, 980-983.
126. Lang, S. M.; Bernhardt, T. M.; Barnett, R. N.; Landman, U. Temperature-Tunable Selective Methane Catalysis on $Au_2^+$: From Cryogenic Partial Oxidation Yielding Formaldehyde to Cold Ethylene Production. *J. Phys. Chem. C* **2011,** *115*, 6788-6795.
127. Lang, S. M.; Frank, A.; Bernhardt, T. M. Comparison of methane activation and catalytic ethylene formation on free gold and palladium dimer cations: Product binding determines the catalytic turn-over. *Catal. Sci. Technol.* **2013,** *3*, 2926-2933.